

## Combined lattice-location-hyperfine-interaction experiment on Se implanted in Fe and Co

P. T. Callaghan, N. J. Stone, and B. G. Turrell\*

Clarendon Laboratory, Oxford, England

(Received 7 January 1974)

The channeling technique has been used to study the lattice location of Se implanted into Fe and Co (hcp) single crystals. For both systems the impurity is found to be fully substitutional at doses of  $5 \times 10^{14} \text{ cm}^{-2}$ . Nuclear-orientation measurements at mK temperatures have been made on implanted  $^{75}\text{Se}$  in Fe and Co polycrystalline hosts. Nuclear magnetic resonance of oriented nuclei (NMR/ON) was observed for  $^{75}\text{Se}$  at 141.6 MHz ( $H_{\text{ext}} = 0$ ) and a resonance-shift experiment yields  $|\mu(^{75}\text{Se})| = (0.67 \pm 0.04)\mu_N$  and  $H_{\text{hf}}(\text{FeSe}) = 690 \pm 50 \text{ kG}$ . For  $\text{CoSe}$  no NMR/ON signal was observed, but the temperature-dependent  $\gamma$  anisotropy is fitted to yield  $H_{\text{hf}}(\text{CoSe}) = +420 \pm 40 \text{ kG}$  or  $-440 \pm 40 \text{ kG}$  although these values make no allowance for possible quadrupole interactions at the hcp lattice site. In the analysis of the  $^{75}\text{Se}$  nuclear-orientation experiment, the  $\delta(E2/M1)$  mixing ratios of the 280- and 265-keV transitions are determined. These results are compared with recent intermediate-coupling collective-model calculations.

### I. INTRODUCTION

In recent years the use of ion implantation as a technique for sample preparation of systems not readily accessible by conventional thermal-diffusion methods has been the subject of extensive experimentation. The necessity of correlating the lattice position of the implant with its particular property under investigation has led to the associated development of impurity-atom location techniques employing the channeling and Rutherford backscattering of charged particles. In this paper, such a combined experiment to measure the hyperfine interaction for Se in Fe and Co is reported. Apart from its interest as an example of the implantation technique, the experiment has intrinsic interest. The magnetic hyperfine interaction in these alloys for different  $4s$ - $4p$  impurities may be expected to show a similar behavior to the striking change from negative to positive fields exhibited by analogous  $5s$ - $5p$  impurities in the series Ag-Cd-In-Sn-Sb-Te-I-Xe. In the  $4s$ - $4p$  series Cu-Zn-Ga-Ge-As-Se-Br-Kr, the interactions for the final members can only be measured using implanted alloys, and results so far have been difficult to interpret because of the coexistence of a variety of impurity sites.

In a recent nuclear-orientation experiment, the average hyperfine field at Br implanted in Fe was measured,<sup>1</sup> but channeling experiments have shown that only 40% of the implanted Br is substitutional.<sup>2</sup> One method of obtaining an estimate of the substitutional hyperfine field at Br in Fe is to make an extrapolation from hyperfine-field systematics at the end of the  $4s$ - $4p$  shell. Especially important, therefore, is a knowledge of the hyperfine field at substitutional Se in Fe.

There is no known value for the solubility of Se in Fe, but Se is known to react with iron to form a

selenide.<sup>3</sup> One might, therefore, expect that it would prove difficult to prepare an  $\text{FeSe}$  alloy by conventional diffusion. The first indication that implanted Se might be a more favorable case came from perturbed angular correlation experiments on the  $\gamma$  cascade in  $^{75}\text{As}$  following the decay of  $^{75}\text{Se}$  implanted into Fe.<sup>4</sup> The study reported here, on identical sources, utilizes low-temperature nuclear orientation combined with NMR to measure the hyperfine interaction of the  $^{75}\text{Se}$  parent.

In Sec. II the lattice location determinations of  $\text{FeSe}$  and  $\text{CoSe}$  are described and an account of the hyperfine interaction measurements is given in Sec. III. Section IV includes a discussion of the  $^{75}\text{As}$   $\gamma$  multipole mixing ratios.

### II. LOCATION OF IMPLANTED SELENIUM

#### A. Samples

In order to be certain that the implanted single crystals to be used in the atom location experiment should have a Se site distribution closely resembling the active samples, it was decided to implant at the same energy (127 keV), and at similar dose ( $1 \times 10^{14} \text{ ions cm}^{-2}$ ), as the active samples (see Sec. III). Inactive implants were done on the Harwell Mk IV separator at 120 keV with Se doses of  $1 \times 10^{14}$  and  $5 \times 10^{14} \text{ cm}^{-2}$ , the latter dose being the minimum at which complete angular scans could be performed in a reasonable time.

The  $5N$  Fe single crystal was obtained from Materials Research Corp., and was cut with the  $\langle 110 \rangle$  axis normal and electropolished in a solution consisting of 5% perchloric acid and 95% glacial acetic acid.<sup>5</sup>

Below  $417^\circ\text{C}$ , the hcp phase of polycrystalline cobalt is thermodynamically stable, and a determination of the hcp fraction at room temperature<sup>6</sup> has shown it to exceed 75% over a wide range of

annealing temperatures and crystallite sizes. Therefore the appropriate cobalt single-crystal structure to use in the CoSe location experiment is hcp. A 4N-purity hcp Co crystal was obtained from Metals Research Ltd., Herts. Two 3 mm  $\times$  2 mm  $\times$  1 mm crystals were cut with the *c* axis at 5° to the surface normal. These were electro-polished in a solution consisting of concentrated HCl and C<sub>2</sub>H<sub>5</sub>OH in equal proportions, and were ultrasonically cleaned in a bath of C<sub>2</sub>H<sub>5</sub>OH.<sup>5</sup>

Both the Fe and Co crystals were implanted with their channeling axes at  $\sim$ 8° to the <sup>80</sup>Se beam direction, so as to avoid channeling and a consequent anomalous implant depth distribution.

### B. Channeling experiment

Atom location using the channeling technique has been discussed extensively elsewhere.<sup>7</sup> For substitutional foreign atoms in a single crystal lattice, the channeled beam interaction yield from some close encounter process such as Rutherford backscattering is attenuated in the same way for both foreign and lattice atoms.<sup>8</sup> In the present experiments, 3.5-MeV <sup>14</sup>N<sup>+</sup> ions were used as the probe beam on the Harwell 5-MV Van de Graaff channeling facility.<sup>9</sup> The beam was collimated to a divergence of  $\pm$ 0.03° and impinged on the single crystal target held in the three-axis goniometer. The goniometer stepping motors allow angle steps as small as 0.01°. Throughout the experiments, the target chamber was kept at a pressure  $\leq$  10<sup>-6</sup> Torr. Figure 1 shows the FeSe 3.5-MeV <sup>14</sup>N backscattering spectrum for an integrated target current of 4.00  $\mu$ C on a 1-mm<sup>2</sup> beam spot. A 100-mm<sup>2</sup> sur-

face barrier detector at 165° and 10 cm from the target was used. The pulse analysis electronics included a pileup rejection system.<sup>10</sup>

The Se and Fe windows are also shown in Fig. 1, the Fe windows being chosen so as to correspond to the depth of the Se implant. The Se depth was determined by comparing the energy of the peak corresponding to backscattering from the Se nuclei of 3.5-MeV <sup>14</sup>N with the energy for backscattering off the surface of amorphous Se. Using the stopping powers given in Ref. 11, the mean projected range and straggling were determined as

$$\bar{R}_p = 350 \pm 40 \text{ \AA}$$

and

$$\Delta\bar{R}_p = 100 \pm 40 \text{ \AA (standard deviation).}$$

Backscattering of 3.5-MeV <sup>14</sup>N from Co<sup>80</sup>Se gave a similar spectrum to that shown in Fig. 1 except that the host energy was slightly higher, since cobalt atoms are heavier than those of iron. A small Cu impurity peak was seen in the FeSe spectrum (see Fig. 1). No such peak was seen in the backscattering from CoSe. Examination of the backscattered <sup>14</sup>N energy spectrum for unimplanted Fe and Co crystals showed that there were no impurity peaks at the energies corresponding to scattering from Se.

A complete angular scan was performed across the  $\langle$ 110 $\rangle$  axis of the  $5 \times 10^{14} \text{ cm}^{-2}$  Fe crystal in a tilting plane at 14° from a  $\{211\}$  plane. The counts in the Se peak were corrected for the projected background drawn in Fig. 1 and normalized to the random line drawn at a tangent to the random counts obtained at  $\pm$ 4.0°. At each angle in the scan, the beam current was adjusted to keep the pileup rate, and hence the Se background level, approximately constant. At the random positions, the beam current was  $\sim$ 0.2 nA, while at the center of the scan it was increased to  $\sim$ 2 nA. The total integrated current in each case was 5.00  $\mu$ C on  $\sim$ 1-mm<sup>2</sup> beam spot.

The results of the Fe  $\langle$ 110 $\rangle$  angular scan are shown in Fig. 2(a). The Se yield closely follows the Fe yield, which indicates that the Se atoms occupy substitutional sites. As a check,  $\chi_0$  (minimum yield) measurements were carried out for the  $\langle$ 111 $\rangle$  and  $\langle$ 100 $\rangle$  axes and the  $\{110\}$  plane. The results are shown in Table I, and the close agreement between the host and impurity yields confirms the substitutional Se location. There exists no off-lattice site [within a Thomas-Fermi (TF) screening distance] for which the  $\chi_0$  value could be so close to the host value for all these channeling directions.

A complete angular scan was also performed across the Co *c* axis at 12° to the nearest major crystal plane in the crystal doped with  $5 \times 10^{14} \text{ cm}^{-2}$  <sup>80</sup>Se. Alignment of the Co crystal was difficult

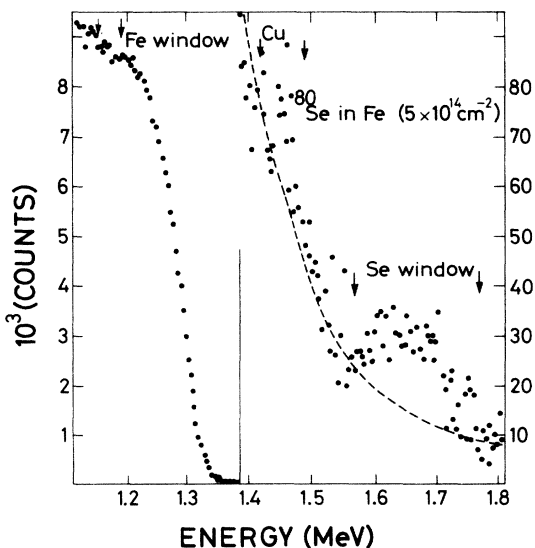


FIG. 1. Backscattered energy spectrum for 3.5-MeV <sup>14</sup>N ions on Se-implanted Fe. The beam is at a few degrees from a  $\langle$ 110 $\rangle$  direction.

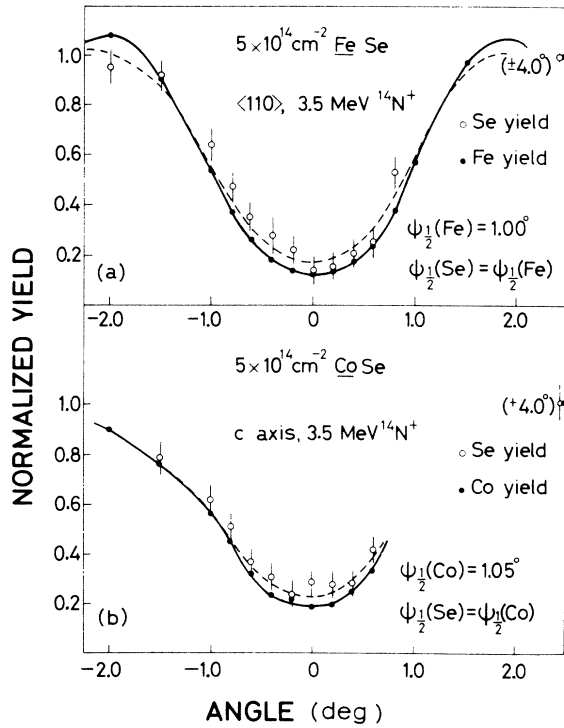


FIG. 2. Normalized backscattering yield as a function of angle for (a) implanted  $FeSe$  near a  $\langle 110 \rangle$  direction, (b) implanted  $FeSe$  near the hcp  $c$  axis.

because the planes which one uses to find the major axis have such weak channeling dips.

In every other respect, the experimental technique and data analysis for this scan were the same as for the Fe  $\langle 110 \rangle$  scan. The results are shown in Fig. 2(b) and, again, indicate a substitutional Se location. Since there exist no other major hcp axes or planes within  $90^\circ$  of the  $c$  axis, it was not possible to confirm this conclusion with other  $\chi_0$  measurements.

In view of the apparent substitutional Se location in both the Fe and Co  $5 \times 10^{14} \text{ cm}^{-2}$  alloys, it would be highly unlikely that any different location would be found for the  $1 \times 10^{14} \text{ cm}^{-2}$  alloys. For this reason, and since  $\chi_0$  measurements at a dose of  $1 \times 10^{14} \text{ cm}^{-2}$  were found from experience to take  $\sim 24$  h of accelerator time, it was decided not to carry out backscattering measurements on the low-dose samples.

The radiation damage introduced into the Co crystal by the implantation is comparatively greater than that introduced into the iron. Taking the lattice spacings<sup>12</sup> for cobalt to be  $c = 4.07$  and  $a = 2.51 \text{ \AA}$ , and for iron  $a = b = c = 2.87 \text{ \AA}$  one may calculate a theoretical minimum yield for the cobalt  $c$  axis and iron  $\langle 110 \rangle$  axis by taking the ratio of the hard-core scattering area to the channel area. Using a scattering area given by  $n f \pi a_{TF}^2$ ,

where  $n$  is the number of boundary strings and  $f$  is the fraction of their area in the channel, it can be shown that

$$\chi_0^{\text{calc}}(\text{Co}) = 0.02 \quad (c \text{ axis}),$$

$$\chi_0^{\text{calc}}(\text{Fe}) = 0.018 \quad (\langle 110 \rangle \text{ axis}).$$

The ratio  $\chi_0^{\text{expt}}/\chi_0^{\text{calc}}$  is 7 for Fe and 10 for Co, which indicates a higher level of radiation damage in Co if one assumes that lattice defects are the dominant cause of dechanneling.

### III. HYPERFINE-FIELD MEASUREMENTS

#### A. NMR/ON of $Fe^{75}Se$

The technique of nuclear magnetic resonance of oriented nuclei (NMR/ON) is performed on radioactive nuclei present as dilute impurities in ferromagnets. Thermal equilibrium nuclear orientation, which has been fully described elsewhere,<sup>13</sup> is used to produce a polarization of the ensemble of nuclear spins whose consequent  $\gamma$ -ray distribution exhibits an anisotropy described by the expression

$$W(\theta) = \sum_{\nu=0}^{\min(2I, 2L)} U_{\nu} F_{\nu} B_{\nu} (\mu H / I k T) P_{\nu}(\cos \theta), \quad (1)$$

where  $I$  is the parent nuclear spin and  $L$  is the multipolarity of the observed transition.  $B_{\nu}$  is the orientation parameter,  $P_{\nu}$  is a Legendre polynomial, and  $U_{\nu}$  and  $F_{\nu}$  are the preceding and observed decay parameters.<sup>14</sup> For a mixed  $L, L^1$  transition, the decay parameters take the form

$$U_{\nu} = \frac{U_{\nu}(L) + \delta^2 U_{\nu}(L^1)}{1 + \delta^2}$$

and

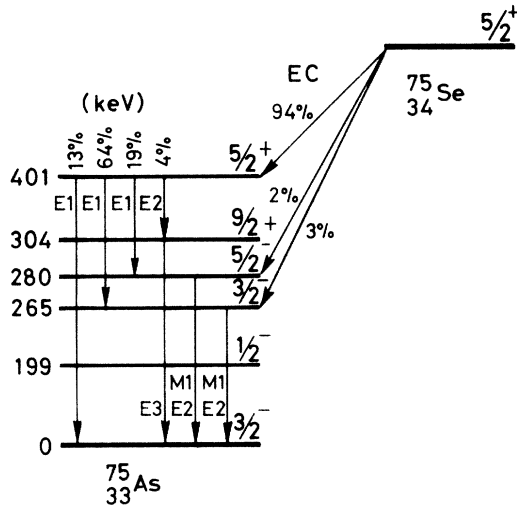
$$F_{\nu} = \frac{F_{\nu}(L, L) + 2\delta F_{\nu}(L, L^1) + \delta^2 F_{\nu}(L^1, L^1)}{1 + \delta^2}, \quad (2)$$

where  $\delta$  is the  $L, L^1$  mixing ratio. In the NMR/ON experiment, the resonance is detected by observing the change in  $\gamma$ -ray count rate along the axis of polarization, as the populations of the  $2I+1$  sub-levels in the hyperfine split ground state are changed by resonant rf absorption.

Radioactive samples of  $^{75}Se$  implanted into polycrystalline Fe and Co were provided by Drentje, whose laboratory in Groningen performed the im-

TABLE I. Aligned to random yields for backscattering of 3.5-MeV  $^{14}N$  from Fe and Se in various channeling directions for implanted  $5 \times 10^{14} \text{ cm}^{-2} FeSe$ .

Channel	$\chi_0$ (Fe)	$\chi_0$ (Se)
$\langle 111 \rangle$	0.08	$0.17 \pm 0.05$
$\langle 100 \rangle$	0.10	$0.15 \pm 0.05$
$\{110\}$	0.28	$0.26 \pm 0.06$

FIG. 3. Decay scheme of  $^{75}\text{Se}$ .

plantations for the  $^{75}\text{As}$  angular correlation experiment. These samples had a Se dose of  $\sim 1 \times 10^{14}$  ions  $\text{cm}^{-2}$  and were implanted at 127 keV. The decay scheme<sup>15</sup> of  $^{75}\text{Se}$  is shown in Fig. 3.  $^{75}\text{Se}$  decays 94% by allowed electron capture from its  $5/2^+$  ground state to the  $5/2^+$  401 keV level in  $^{75}\text{As}$ . For such a transition, the electron angular momentum may be  $j_\beta = 0$  (Fermi) or  $j_\beta = 1$  (Gamow-Teller). The spins and  $\gamma$  multiplicities in the  $^{75}\text{As}$  daughter are all well known. The 265-keV and 280-keV  $\delta(E2/M1)$  mixing ratios have been measured by Becker and Steffen<sup>16</sup> and Raeside *et al.*,<sup>17</sup> yielding the values shown in Table II. A nuclear-orientation experiment on  $^{75}\text{Se}$  implanted into iron has, therefore, several objects. First, if the resonant frequency for the substitutional  $^{75}\text{Se}$  nuclei can be found, the value for  $\mu H_{\text{hf}}/I$  so determined can be used to fit the temperature-dependent anisotropy of the pure

dipole transitions at 121, 136, and 401 keV, to yield information about the angular momentum character of the  $5/2^+ \rightarrow 5/2^+$  electron capture. The 265 and 280 keV  $\gamma$  anisotropies may then be fitted to yield new values for  $\delta(E2/M1)$ . Secondly, and more importantly, the values of  $\mu$  and  $H_{\text{hf}}$  may be determined separately by observing the shift of the resonant frequency,

$$\nu = \mu (Fe^{75}\text{Se}) | \vec{H}_{\text{hf}} + \vec{H}_{\text{ext}} | / I h, \quad (3)$$

on increasing the applied field  $H_{\text{ext}}$ .

The implanted polycrystalline  $Fe^{75}\text{Se}$  samples consisted of a thin ( $\sim 200 \mu\text{m}$ ) Fe sheet soft-soldered to a 2-mm-thick copper-backing strip prior to implantation. The implanted region was a long strip about 3 mm wide whose implantation dose of  $\sim 1 \times 10^{14} \text{ cm}^{-2}$  was estimated from a knowledge of the initial source specific activity, and by assuming a separator efficiency of  $2 \times 10^3$ .<sup>18</sup> Two samples, each 3 mm wide and 10 mm long, were cut from the implanted region and were Woods-metal soldered with their implanted faces outward on opposite sides of the salt-pill cold finger; care was taken to not heat them much above the meltingpoint of the solder. A small  $Fe^{60}\text{Co}$  thermometric source was soldered nearby.

The Ge(Li) spectrum is shown in Fig. 4, and the temperature-dependent anisotropies for the 136 and 280-keV gamma transitions are shown in Fig. 5. In these measurements the sample was polarized in an external field of 5 kG. All temperatures have been corrected for  $H_{\text{ext}}$ .

Using  $\pm 400$ -kHz modulation, a scan was made between 105 and 145 MHz, spending 400 sec at each 1-MHz step. For each step a complete Ge(Li) spectrum was accumulated. At 142 MHz, a destruction of anisotropy was seen simultaneously on the 136, 280, and 401-keV  $\gamma$  rays, measuring 8, 6, and 3 standard deviations, respectively. In a

TABLE II. Comparison of  $\delta(E2/M1)$  mixing ratios for the 265- and 280-keV transitions.

Method	$\delta(E2/M1)_{265}$	$\delta(E2/M1)_{280}$	Reference
Nuclear orientation	$-0.18 \pm 0.02$	$-0.35 \pm 0.03$	this work
	$14 \pm 1$	$-1.4 \pm 0.1$	
$\gamma\gamma$ angular correlation	$-0.05 \pm 0.03,$ $+4.7 \pm 0.05$	$-0.39 \pm 0.02$ $-1.28 \pm 0.04$	Raeside <i>et al.</i> <sup>a</sup>
	$-0.043 \pm 0.06^b$	$-0.48 \pm 0.03^b$	Speidel <i>et al.</i> <sup>c</sup>
Resonance scattering	$-0.01 \pm 0.04^b$	$-0.42 \pm 0.08^b$	Langhoff and Schumacher <sup>d</sup>
$e^-\gamma$ angular correlation	$-0.04 \pm 0.02^b$	$-0.25 \pm 0.01^b$	Vignau <i>et al.</i> <sup>e</sup>

<sup>a</sup>Reference 17.<sup>b</sup>Only one root given.<sup>c</sup>Reference 20.<sup>d</sup>Reference 21.<sup>e</sup>Reference 22.

separate run, the resonance line shape was obtained by observation of the 136-keV  $\gamma$  ray alone. A modulation amplitude of 370 kHz was used with the frequency stepped 0.2 MHz every 400 sec. The results of sweeps in both directions are shown in Fig. 6. In order to obtain a relaxation-time estimate, it was necessary to use a shorter counting interval. Consequently, a NaI detector was used with a window on the 401-keV transition, the best resolved peak. Successive 100-sec counts were taken with the modulation removed. The nuclear spin-lattice relaxation time at  $1/T = 50 \text{ K}^{-1}$  was found to be  $T_1 = 130 \pm 50 \text{ sec}$ . Such a relaxation time has no significant influence on the NMR/ON line shape when the count time is 400 sec. Consequently the data of Fig. 6 have been fitted without making allowance for relaxation.<sup>19</sup> The full width at half-maximum is 1.00 MHz, the integrated destruction is 70%, and the center frequency is  $142.1 \pm 0.1 \text{ MHz}$  at 2.32-kG applied field. Such a large destruction and narrow linewidth, comparable with typical values for diffused NMR/ON sources, strongly supports the notion that the  $^{75}\text{Se}$  occupy unique substitutional sites.

In an independent measurement of  $\mu(^{75}\text{Se})$  and  $H_{\text{hf}}(\text{FeSe})$ , the center of the resonance line was found under 11.6 and 20.9 kG applied field, in addition to that already determined at 2.32 kG. The high field represented a practical upper limit for the nuclear-orientation cryostat polarizing field, since at higher fields difficulties arose because of the stray field warming the salt pill, and because of the excess heating of the bath due to Joule dissipation in the leads.

Using the three values of resonant frequency and applied field, a least-squares fit was used to yield

$$\nu(\text{Fe}^{75}\text{Se}) = 141.6 \pm 0.1 \text{ MHz} \quad (\text{at } H_{\text{ext}} = 0)$$

$$|\mu(^{75}\text{Se})| = (0.67 \pm 0.04)\mu_N$$

$$H_{\text{hf}}(\text{FeSe}) = +690 \pm 50 \text{ kG}.$$

A more accurate determination of  $\mu(^{75}\text{Se})$  by any

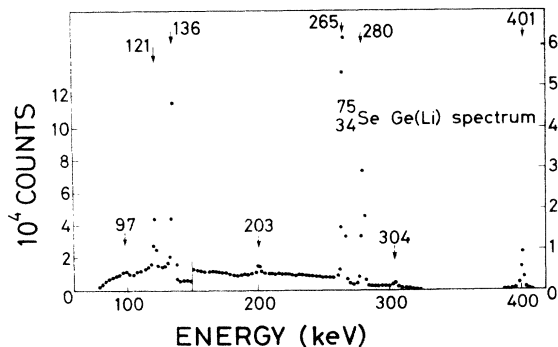


FIG. 4. Ge(Li) spectrum of  $^{75}\text{Se}$ . The source was the implanted nuclear-orientation specimen.

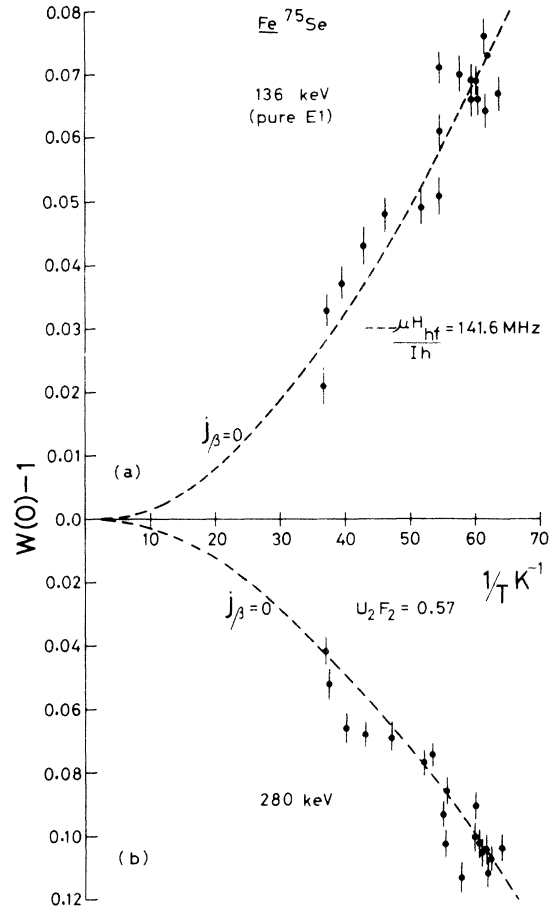


FIG. 5. (a) Temperature-dependent normalized axial anisotropy for the 136-keV  $\gamma$  from implanted  $^{75}\text{FeSe}$ . The fit uses the known decay parameters and shows the close agreement with the hyperfine splitting determined in the resonance experiment. (b) Temperature-dependent axial anisotropy for the admixed 280-keV transition. The measured hyperfine splitting is used to fit the data so as to yield the decay parameters.

means will fix  $H_{\text{hf}}(\text{FeSe})$  more accurately.

The anisotropy data for the 121, 136, and 401 keV (pure E1) transitions were fitted using

$$\begin{aligned} \mu(H_{\text{hf}} + 5 \text{ kG})/Ih &= 141.6 \text{ MHz} \\ &+ (0.67 \times 5.0 \mu_N \text{ kG})/Ih, \quad (4) \end{aligned}$$

where  $I = \frac{5}{2}$ . The computed curves agree well with the measured transition anisotropies if one takes the preceding electron capture as pure  $j_B = 0$  (Fermi). The fit for the 136-keV transition whose anisotropy is most accurately determined is shown in Fig. 5(a). One may place limits on the square of the  $[(j_B = 1)/(j_B = 0)]$  mixing ratio,  $\Delta$ , by using the measured 136-keV anisotropy, so that

$$0 \leq \Delta^2 \leq 0.05.$$

A measurement of the  $F_2$  coefficients for the 280-

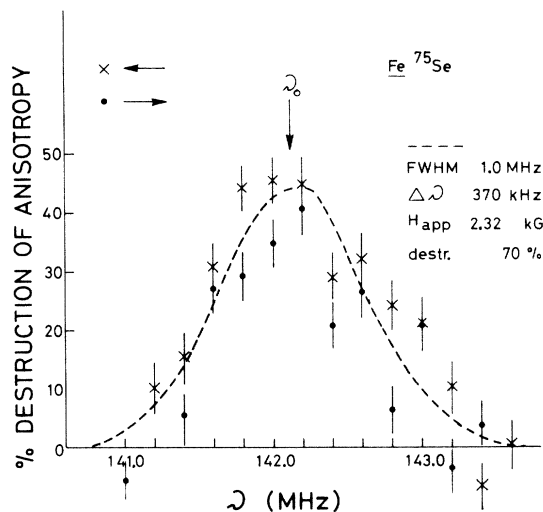


FIG. 6. NMR/O N of implanted  $^{75}\text{FeSe}$ . The Gaussian fit is a mean for both sweep directions.

and 265-keV transitions can then be made by taking the value of  $U_2$  implied by the determination that  $j_\beta$  is zero. For the 280-keV transition,  $U_2 F_2 = +0.57 \pm 0.02$ , while for the 265-keV transition,  $U_2 F_2 = 0.08 \pm 0.02$ . (The  $\nu = 4$  terms may be neglected, since  $B_4 \lesssim 0.01 B_2$  at  $1/T = 60 \text{ K}^{-1}$ .) The values thereby implied for  $\delta(E2/M1)$  are shown in Table II, and for the 280-keV transition they appear to be in good agreement with earlier measurements. Figure 5(b) shows the fit to the 280-keV anisotropy. The poorer 265-keV result is attributable to the difficulty in finding the true background level under the peak when calculating gamma anisotropy. Because of scattered lower-energy gammas from the 280-keV transition (whose anisotropy has opposite sign), the background under the 265-keV peak has a strong temperature dependence.

#### B. Nuclear orientation of $\text{Co } ^{75}\text{Se}$

The polycrystalline hcp Co sample used in this experiment was similar in dimensions to the  $\text{Fe } ^{75}\text{Se}$  sample and, like it, had a selenium dose of  $1 \times 10^{14} \text{ cm}^{-2}$ . Since cobalt is more difficult to magnetize than iron, it is necessary to use a higher polarizing field to ensure saturation of the gamma anisotropy. In the present experiment, 12 kG was used, a field sufficient to give saturation better than 95%.<sup>23</sup> The results of the  $\text{Co } ^{75}\text{Se}$  nuclear-orientation experiment, and of the 136- and 280-keV transitions whose anisotropies are most accurately determined are shown in Fig. 7. The anisotropy data have been fitted with a field  $H_{\text{eff}}(\text{CoSe}) = 0.62 H_{\text{hf}}(\text{FeSe})$ , where  $H_{\text{eff}}$  includes the 12-kG applied field  $H_{\text{ext}}$ , and good agreement is found for all four major transitions. After correcting for  $H_{\text{ext}}$  one obtains

$$H_{\text{hf}}(\text{CoSe}) = +420 \pm 40 \text{ kG} \text{ or } -440 \pm 40 \text{ kG}.$$

Such a field at  $^{75}\text{Se}$  implies an NMR frequency of  $\sim 90 \text{ MHz}$ . A resonance search was mounted in a manner exactly similar to that described for iron, except that a high polarizing field of 9 kG was used to maintain high gamma anisotropy without losing greatly on the hyperfine enhancement factor  $1 + (H_{\text{hf}}/H_{\text{ext}})$ . In a sweep from 85 to 111 MHz, no significant destruction of anisotropy was seen on any of the 136, 280, or 401-keV transitions. Only 10 to 15 standard deviations of anisotropy were available, and so a signal of at least 30% destruction would have been necessary to observe resonance. In a previous experiment by Barclay<sup>24</sup> on  $^{60}\text{Co}$  in hcp cobalt metal, no resonance was seen. It is probable that the quadrupolar line broadening due to a crystal-field gradient at the noncubic lattice site is responsible for the difficulty experienced in observing NMR/O N. The presence of a quadrupole term in the Hamiltonian causes an effective magnetic field  $\bar{H}_{\text{hf}} \neq H_{\text{hf}}$  to be measured in a nuclear-orientation experiment. It has been shown<sup>25</sup> that, for a nuclear quadrupole moment  $Q$  in an electric

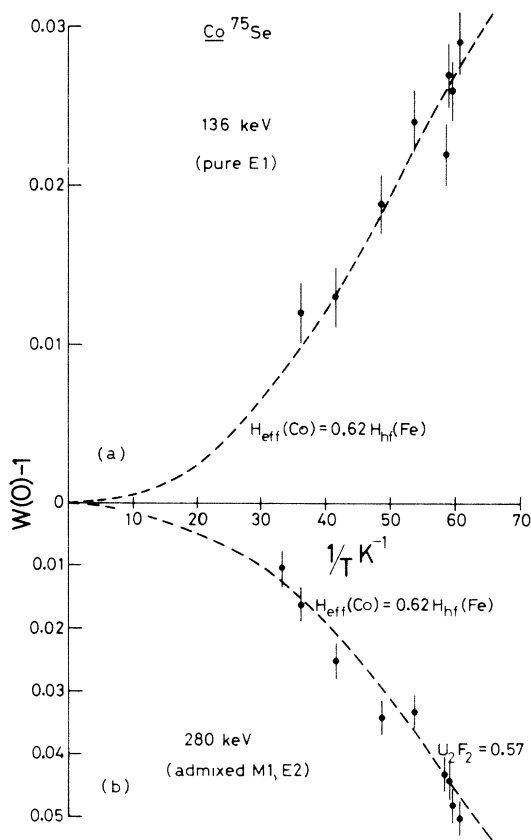


FIG. 7. (a) Temperature-dependence anisotropy for the 136-keV gamma from implanted  $\text{Co } ^{75}\text{Se}$ . The data are fitted to yield  $H_{\text{eff}}(\text{Co})$ . (b) Temperature-dependent anisotropy for the 280-keV transition. The decay parameters determined from the  $\text{Fe } ^{75}\text{Se}$  experiment are used.

field gradient  $V_{zz}$ , the effective hyperfine field determined by nuclear orientation may differ from the true field up to a factor

$$(\bar{H}_{hf}/H_{hf})(T \rightarrow 0) = 1 + 3eQV_{zz}/4\mu H_{hf}. \quad (5)$$

### C. Other $Fe^{75}Se$ samples

A nuclear-orientation experiment was also carried out using the angular correlation sample for which the  $^{75}As$  daughter was found to experience the substitutional field. This sample was kindly provided by the Tata Institute, Bombay, and had also been prepared on the Groningen separator. Not surprisingly, since the conditions of implantation had been identical with those of the  $Fe^{75}Se$  samples used in the NMR/ON experiments, an identical anisotropy was measured for the major transitions.

A sample of  $Fe^{75}Se$  was also prepared by conventional diffusion.  $^{75}Se$  activity was obtained from the Radiochemical Center, Amersham, in the form of 10-mCi  $mg^{-1}$  sodium selenite. A small amount of this activity was evaporated onto the surface of a 3-mm  $\times$  10-mm  $\times$  100- $\mu m$  99.999%-pure Fe foil, sealed *in vacuo* in quartz, and diffused for 10 h at 1300  $^{\circ}C$ . In order to ensure removal of any remaining surface activity, the resulting sample was etched three times for 1 min in 1N  $HNO_3$  and, between each etch, was polished with fine emery paper. The sample was then soldered with Woods metal to the chrome alum salt-pill cold finger, cooled, and polarized in 5 kG. This sample was considerably less active than the implanted sources and, when mounted on the apparatus with the  $Fe^{60}Co$  thermometer, a proportionally much greater background due to degraded  $^{60}Co$  radiation was observed under the 121- and 136-keV peaks.

All the gamma anisotropies for the diffused sample were found to be reduced in comparison with the implanted source, thus indicating a lower average hyperfine field. It is unlikely, in view of the surface removal during etching, that any active  $^{75}Se$  remained on the surface. If one assumes that the Se atoms occupy a unique lattice site and experience a purely magnetic interaction, then the 280- and 401-keV anisotropies (the most accurately determined) indicate that the Se hyperfine field is  $(75 \pm 5)\%$  of the substitutional field. More likely, however, is that some or all of the Se has formed local precipitates of iron selenide in which the hyperfine field is lower than at the lattice site.

## IV. INTERPRETATION AND CONCLUSIONS

The combined atom-location-NMR/ON experiment on implanted selenium shows the interdependence of the techniques. Atom location using chan-

TABLE III. Comparison of measured and calculated M1, E2 transition rates for the 265- and 280-keV transitions in  $^{75}As$ . All transition rates are in units of  $10^3 \text{ sec}^{-1}$ , and for the 265-keV transition the experimental rates refer to those measured by Raeside *et al.*

Transition	Parent level	$1/T(M1)_{s.p.}$	$1/T(E2)_{s.p.}$	$1/T(M1)_{expt.}$	$1/T(E2)_{expt.}$	R (M2)	E (E2)	$1/T(M1)_{coll.}^a$	$1/T(E2)_{coll.}^a$
265 keV $\frac{3}{2}^- \rightarrow \frac{3}{2}^-$	265 keV $12 \times 10^{-12} \text{ sec}$	520	0.13	58	0.14	8	1.1	12	0.80
280 keV $\frac{5}{2}^- \rightarrow \frac{3}{2}^-$	280 keV $0.42 \times 10^{-9} \text{ sec}$	620	0.025	1.47	0.18	400	7	0.080	0.040

<sup>a</sup>From Ref. 27.

neling has revealed the substitutional character of implanted  $FeSe$  and  $CoSe$  alloys. The resonant destruction of nuclear orientation has yielded the hyperfine field at selenium in iron, as well as the moment of  $^{75}Se$ , and the measurement of the temperature-dependent  $\gamma$  anisotropy for oriented  $Fe^{75}Se$  has given additional data about the electromagnetic transitions between excited states of  $^{75}As$ . Without the channeling experiment, the nuclear-orientation measurements would have been difficult to interpret. For an implanted alloy there is no reason, *a priori*, to assume that the impurity atoms occupy unique sites in the lattice. In this study, it is the evidence of the channeling experiment which has allowed the assignment of a unique hyperfine field (determined by NMR/ON) to each radioactive selenium atom in the  $Fe^{75}Se$  alloy.

The nuclear physics aspects of the selenium study thus rest fundamentally upon the hyperfine-field measurements and the alloy structure determination. These results fix the form of the  $B_2$  coefficients used in the analysis of the gamma anisotropy. The 280- and 265-keV  $E2/M1$  mixing ratios determined in the nuclear-orientation experiment can be used to test possible eigenstates for the 280- and 265-keV levels in  $^{75}As$ . The available odd-quasiparticle states for these two levels are primarily  $1f_{5/2}$ ,  $2p_{3/2}$  and  $2p_{1/2}$ . By an argument based on the maximum likely  $E2$  transition rate, one may eliminate the larger of the two solutions for  $\delta(E2/M1)$  for both the 280- and 265-keV transitions.

Paradellis and Hontzeas<sup>26</sup> have made collective model calculations (in intermediate coupling) for  $^{75}As$ . They choose a coupling strength parameter in order to give the best agreement between calculated and experimental excited-state energy levels. They then calculate  $E2$  and  $M1$  transition rates for the 280-keV ( $\frac{5}{2}^- \rightarrow \frac{3}{2}^-$ ) and 265-keV ( $\frac{3}{2}^- \rightarrow \frac{3}{2}^-$ ) transitions. With single-particle states, the 280-keV transition is  $l$ -forbidden for the  $M1$  multipole. The size of the observed  $M1$  reduction factor will therefore give a fair indication of deviation from pure  $f_{5/2}$  character of the 280-keV level. In Table III, the single-particle and collective model transition rates, according to Ref. 27, are shown. The experimental rates shown were computed using level lifetimes and (insignificant) conversion coefficients taken from nuclear data sheets.<sup>15</sup> For the 280-keV transition, the large  $M1$  reduction factor indicates a fairly pure quasiparticle  $f_{5/2}$  character. The collective calculation, however, gives too much *single-particle* character to the 280-keV level, as witnessed by the fact that the calculated  $M1$  and  $E2$  transition rates are both too small. In contrast, the collective model gives too much  $E2$  intensity and too little  $M1$  intensity for the 265-keV level. For this  $l$ -al-

lowed  $M1$  transition, these two discrepancies indicate too much *collective* character in the calculated 265-keV eigenstate.

Clearly, an adjustment of the state independent collective parameters such as the surface coupling strength or the phonon excitation energy cannot satisfy the eigenstate requirements of both the 280- and 265-keV levels, whose predicted collective characters are too small and too large, respectively. It is possible that the model would give better results if the quasiparticle basis functions were expanded to include other states (for example, the  $1f_{7/2}$  proton hole state).

Agreement between some chosen model and experiment is generally easier to achieve for a static magnetic moment than for electromagnetic transition rates, whose values may range over many orders of magnitude. The pairing-plus-quadrupole model predicts a  $^{75}Se$  ground-state moment of  $+0.77\mu_N$ ,<sup>28</sup> in fair agreement with the value of  $\pm(0.67 \pm 0.04)\mu_N$  found in the present experiment.

The experiment has also yielded the sign and size of the hyperfine field at Se in Fe, a result which is significant because of the large magnitude of the field at Se ( $\sim 700$  kG). Full interpretation of the  $CoSe$  nuclear-orientation experiment is difficult while uncertainty about the presence of a quadrupole contribution to the Hamiltonian exists. An NMR/ON experiment with polycrystalline *cubic* cobalt implanted with  $^{75}Se$  could help to throw light on this problem. Since cubic single crystals are difficult to prepare, a location experiment on implanted Se in the fcc metal could not be used to test that the Se is substitutional, but an observation of NMR with a large destruction would give a fair indication.

The preparation of substitutional  $FeSe$  by implantation is especially interesting in the light of the nuclear-orientation experiment on diffused  $Fe^{75}Se$  whose  $\gamma$  anisotropy indicated that the Se atoms did not all occupy "good sites." Previous implantations on other systems have only produced substitutional alloys where the impurity was, in any case, able to be placed on the lattice site by thermal diffusion. Examples of such systems are  $FeSb$  and  $FeAu$ , whose implanted alloys have been shown (using channeling) to be substitutional.<sup>9</sup> The channeling technique should therefore be used to test whether or not it is possible to prepare by implantation substitutional alloys with otherwise insoluble impurities (e.g.,  $FeTe$ ).

#### ACKNOWLEDGMENTS

The authors would like to thank Professor H. de Waard and Dr. S. Drentje for sending us the  $^{75}Se$  implants. One of us (P. T. C.) acknowledges the support of a United Kingdom Commonwealth Scholarship. B. G. T. wishes to thank the Clarendon Laboratory for the hospitality shown him during his visit.



- \*Department of Physics, University of British Columbia, Vancouver 8, B. C., Canada.
- <sup>1</sup>P. T. Callaghan, N. J. Stone, and R. B. Alexander (unpublished).
- <sup>2</sup>R. B. Alexander, P. T. Callaghan, and J. M. Poate, Phys. Rev. B (to be published).
- <sup>3</sup>M. Hansen, *Constitution of Binary Alloys* (McGraw-Hill, New York, 1958).
- <sup>4</sup>R. C. Chopra and P. N. Tandon, Phys. Status Solidi B 53, 373 (1972).
- <sup>5</sup>N. J. McG. Tegart, *The Electrolytic and Chemical Polishing of Metals in Research and Industry*, 2nd ed. (Pergamon, London, 1959).
- <sup>6</sup>C. R. Houska, B. L. Auerbach, and M. Cohen, Acta Metall. 8, 81 (1960).
- <sup>7</sup>See, for example, B. I. Deutch, in *Hyperfine Interactions in Excited Nuclei*, edited by G. Goldring and R. Kalish (Gordon and Breach, London, 1971), p. 137 and references therein; R. B. Alexander, N. J. Stone, D. V. Morgan and J. M. Poate, *ibid.*, p. 229.
- <sup>8</sup>R. B. Alexander and J. M. Poate, Radiat. Effects 12, 211 (1972).
- <sup>9</sup>R. B. Alexander, Atomic Energy Research Establishment Report No. AERE-R-6849, July, 1971 (unpublished).
- <sup>10</sup>R. A. Boie and H. P. Lie, private communication (unpublished).
- <sup>11</sup>L. C. Northcliffe and R. I. Schilling, Nucl. Data Tables 7, 233 (1970).
- <sup>12</sup>R. W. G. Wyckoff, *Crystal Structure* (Interscience, New York, 1963), Vol. 1.
- <sup>13</sup>S. R. De Groot, H. A. Tolhoek, and W. J. Huiskamp, *Alpha-, Beta- and Gamma-ray Spectroscopy*, edited by K. Siegbahn (North-Holland, Amsterdam, 1965), Vol. 2, p. 1199.
- <sup>14</sup>R. J. Blin-Stoyle and M. A. Grace, Handb. Phys. 42, 555 (1957).
- <sup>15</sup>Nuclear Data Sheets, B-6-80 (1967).
- <sup>16</sup>A. J. Becker and R. M. Steffen, Phys. Rev. 180, 1043 (1969).
- <sup>17</sup>D. E. Raeside, M. A. Ludington, J. J. Reidy, and M. L. Wiedenbeck, Nucl. Phys. A 130, 677 (1969).
- <sup>18</sup>S. Drentje (private communication).
- <sup>19</sup>P. T. Callaghan and N. J. Stone, Phys. Lett. B 40, 84 (1972).
- <sup>20</sup>K. H. Spiedel, D. Kolb, K. Mittag, J. Voss, B. Wolbeck, G. Dammertz, and K. G. Plinger, Nucl. Phys. A 115, 421 (1968).
- <sup>21</sup>H. Langhoff and M. Schumacher, Phys. Rev. 155, 1246 (1967).
- <sup>22</sup>H. Vignau, A. Moco-roa, R. Othaz, and N. Baade, Nucl. Phys. A 110, 56 (1968).
- <sup>23</sup>P. D. Johnston, D. Phil. thesis (University of Oxford, 1972) (unpublished).
- <sup>24</sup>J. A. Barclay, Ph.D. thesis (University of California, Berkeley, 1969), Report No. UCRL 18986 (1969) (unpublished).
- <sup>25</sup>P. D. Johnston, R. A. Fox, and N. J. Stone, J. Phys. C 5, 2077 (1972).
- <sup>26</sup>T. Paradellis and S. Hontzeas, Can. J. Phys. 49, 1750 (1971).
- <sup>27</sup>S. Moszkowski, in *Alpha-, Beta- and Gamma-ray Spectroscopy*, edited by K. Siegbahn (North-Holland, Amsterdam, 1956).
- <sup>28</sup>L. S. Kisslinger and R. A. Sorenson, Rev. Mod. Phys. 35, 853 (1963).